Transition from during- to post-collision multifragmentation in cluster surface impact

A. Kaplan,* A. Bekkerman, B. Tsipinyuk, and E. Kolodney
Department of Chemistry, Technion–Israel Institute of Technology, Technion City, Haifa 32000, Israel
(Received 17 December 2008; published 17 June 2009)

Multifragmentation of C_{60}^- was studied by measuring the kinetic energies of outgoing C_n^- ($n=2-12$) fragments following C_{60}^- collisions with a gold surface at sub-keV impact energies. We observe the transition from a multifragmentation with common average energy for all fragments ("during-collision" event) to a one with a common average velocity for all fragments ("post-collision" event). The energy distributions for both multifragmentation modes were successfully modeled by treating the fragmenting cluster as a hot "gas" consisted of various C_n fragments and moving with some center of mass velocity.

DOI: 10.1103/PhysRevB.79.233405 PACS number(s): 68.49.Df, 36.40.Qv, 34.50.−s

Fragmentation modes of highly energized microscopic systems, ranging from large macromolecular ions to hot atomic nuclei, are of fundamental physical interest. Their importance is quite often related with the universal patterns revealed and shared by the measured distributions (mass, energy, etc.).[1] These patterns may be applicable for interpreting and predicting fragmentation processes of different objects over very large scales of size and energy.[2,3] Of special interest in this context are multiparticle breakup (multifragmentation) phenomena which were studied already for several molecular species but mainly in the complete impact disintegration limit (shattering), where the projectile is shattered into its smallest constituents. The so-called shattering transition[4–6] from the region of delayed evaporationlike emission of elementary subunits to complete disintegration was observed so far in weakly bound clusters such as $(NH_3)_nH^+$ ($n=4-40$),[6] $I_2(CO_2)_n^-$ ($n=1-50$),[7] antimony clusters $Sb_n^+(n=3-12)$,[8] and also covalent molecular ions such as $Si(Cd_3^+)$,[9] peptide ions,[10] and fullerenes.[11–13] Fullerene molecules and C_{60} specifically have recently turned into a model system for studying different types of fragmentation phenomena following extreme collisional and optical excitations.[14–16] Shattering-type fragmentation was reported by Beck *et al.*[11] for C_{60}^+ ions impacting a graphite surface over the 200–1800 eV energy range based on the evolution of mass distributions alone. The common assumption in the literature is that surface-impact-induced multifragmentation event is completed when the fragments are still in close contact with the surface. This should result in uncorrelated velocities of the outgoing fragments. However, since the reported experimental characterization of these fragments is very limited, not much is known about the actual dynamics of the multifragmentation event. Recently we have shown that the sub-keV multifragmentation of C_{60}^- impacting a gold surface at near-grazing incidence is a fully correlated event, where all scattered C_n^- fragments have nearly the same velocity.[12,13] Here we show that by changing the scattering angle Ψ by 90°, from near grazing ($\Psi=45°$) to near normal ($\Psi=135°$), we observe a dramatic transition from a common-velocity multifragmentation event to a common-energy one (with corresponding kinetic energy losses of 60% and over 99%). Our measurements thus provide information about fragmentation modes which are intermediate between on-flight unimolecular decay and complete shattering at the surface. Interestingly, the two (seemingly) very different multifragmentation modes are described within a single model based on the assumption that the species leaving the surface is a superhot precursor composed of loosely interconnected C_n groups. The actual multifragmentation event can therefore be treated as an expansion/evaporation process of the C_n groups off the outgoing precursor, which occur either away from the surface or at the surface.

The experimental setup was described before.[13] Briefly, C_{60}^- anions were accelerated to kinetic energies of 300–900 eV and collided with an atomically clean polycrystalline gold surface maintained under UHV conditions. C_{60}^- ion beam purity (99.99%) and energy width ($\leq$0.6 eV) were measured using an online mass filter equipped with retarding field energy analyzer. Surface preparation procedures were as described before.[13] In order to assure surface cleanliness and avoid C_{60} sticking, surface temperature was kept at 950 K. The scattering configuration is that of a rotating surface and a fixed detector which could be positioned at two different scattering angles $\Psi=45°$ (near-grazing incidence) or $\Psi=135°$ (near-normal incidence) given by $\Psi=\pi-(\theta_i+\theta_r)$ with incidence angle θ_i and reflection angle θ_r both defined with respect to the surface normal. Mass-resolved energy and incidence-angle dependences of scattered C_n^- fragments were measured by a mass-spectrometer equipped with an on-axis retarding field energy analyzer. All kinetic energy distributions (KEDs) were measured under completely field-free conditions and fully screened flight path of the fragments ion to the energy analyzer.

A shattering-type fragmentation was observed for both near-grazing ($\Psi=45°$) and near-normal ($\Psi=135°$) collisions. One of its main characteristics in C_{60}^--surface impact is odd/even (n-numbered) C_n^- mass distributions as reported before.[11–13] Note that under strict grazing incidence (1°–4°) no shattering behavior was observed.[15,16] Here, a clear shattering threshold, a sharp rise in the total yield of small C_n^- ions ($n=2-22$ for $\Psi=45°$ and $n=2-15$ for $\Psi=135°$) as a function of E_o, was observed. The shattering threshold for $\Psi=45°$ was found to be at $E_o\approx150$ eV, followed by a sharp rise of the integrated C_n^- signal by 2 orders of magnitude increase in the integrated C_n^- signal over the $E_o=150-350$ eV range gradually approaching a plateau region at 900 eV.[13] For $\Psi=135°$, we observe an even more dramatic behavior, resembling a phase transition curve: a threshold at $E_o\approx80$ eV, 2 orders of magnitude steep rise over the $E_o=80-150$ eV range, and then a relatively sharp transition to a plateau region extending up to 900 eV. It should be noted that the low-threshold value measured for both scattering

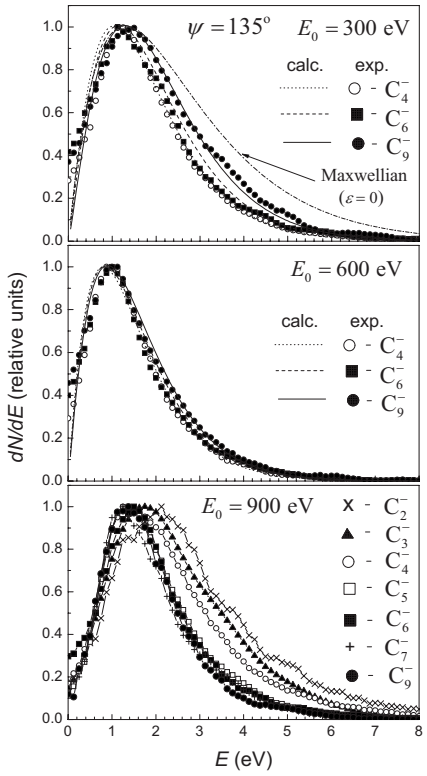

FIG. 1. Kinetic energy distributions of scattered C_n^- fragment anions following impact of C_{60}^- on a gold surface with energies E_0=300, 600, and 900 eV at near-normal incidence (Ψ=135° and θ_i=20°). Both measured and calculated (lines) distributions are shown. The calculated distributions are given only for E_0=300 and 600 eV. A single pair of parameters (kT and ε) was best fitted (see text) for each E_0 value (a complete family of distributions). All distributions are normalized to the same peak intensity.

angles, but especially for Ψ=135° (with respect to the full cohesion energy of C_{60}, estimated ~500 eV),[13] supports a description of the results presented here in terms of a multifragmentation process into a few relatively large fragments. This description seems to be more appropriate here than a complete shattering into the smallest constituents as observed for weakly bound clusters.[6]

Figure 1 shows the kinetic energy distributions of the C_n^- fragment anions scattered at an angle of Ψ=135° (θ_i =20±1°) for impact energies E_o=300 eV ($E_{0\perp}$=265 eV, n=4,6,9), E_o=600 eV ($E_{0\perp}$=530 eV, n=4,6,9), and E_o =900 eV ($E_{0\perp}$=795 eV, n=2–7,9), where $E_{0\perp}$ =$E_o \cos^2 \theta_i$. Generally, all KEDs peak at most probable energies E_{mp} in the range of 1–1.5 eV, except for C_2^-, C_3^-, and C_4^- at E_o=900 eV with E_{mp}≈2 eV. The full width at half maximum (FWHM) for all KEDs is roughly twice their E_{mp} values. A closer inspection of Fig. 1 reveals clear trends between KEDs of different C_n^- measured for a given E_o value (KEDs family) and also evolution of these trends with increase in E_o. At E_o=300 eV the KEDs are getting broader with an increase in the fragment ion size, namely, the C_9^- KED is the broadest one. This trend is getting weaker, but still persists at E_o=600 eV (e.g., the C_9^- KED is still the broadest one). However, when E_o is increased to 900 eV the trend is completely reversed; the C_9^- KED is now the narrowest one while the KEDs for C_4^-, C_3^-, and C_2^- (where the effect is most pronounced) gradually become broader.

In order to understand and to model the (practically) common-energy KEDs for C_n^- fragments (for $n \geq 4$) scattered at near-normal (Ψ=135°) configuration, we will use the clear conclusion drawn from the former common-velocity observation for all C_n^- fragments scattered at near-grazing (Ψ=45°) configuration.[13] Namely, all fragments originate from a common parent (precursor) species. It was proposed that the precursor species for "post-collision" multifragmentation is a scattered C_{60}^- with center of mass (CM) velocity V_{cm} and so highly internally excited that it looses its intrinsic structure and can be considered as a superhot ensemble of 60 carbon atoms which temporally organize into a cluster of C_n groups, loosely interconnected but tightly confined. Both temperature T of this hot ensemble and its V_{cm} define the kinetic energy distributions of the C_n fragments which "evaporate" from the ensemble. Regarding the issue of possible charge exchange processes, we have shown previously,[12,13] that the origin of the negatively charged fragments is indeed a multifragmentation of the superhot C_{60}^- precursor sufficiently far away from the surface such that direct fragment-surface charge exchange is negligible. Specifically, a lower limit of 18 Å was estimated for the distance of formation for C_5^- at 300 eV impact energy.

Assuming a Maxwellian velocity distribution for the different C_n groups *within* the precursor species (in its CM frame) one can write a flux-velocity distribution for the C_n groups (dN_n/dV) in the laboratory frame within a small solid angle $\Delta\Omega$,

$$\frac{dN_n}{dV} = A(nm)^{3/2}V^3 \exp\left[-\frac{nm(V-V_{cm})^2}{2kT}\right], \qquad (1)$$

where $A=n_o\Delta\Omega/(2\pi kT)^{3/2}$, n_o is the volume density of C_n groups, m is the mass of a carbon atom, k is the Boltzman constant, and $\Delta\Omega=\pi\alpha^2$ with α as the angular collection aperture of the experimental setup. The corresponding flux-energy distribution is given by

$$\frac{dN_n}{dE} = 2A(nm)^{-1/2}E \exp\left[-\frac{(\sqrt{E}-\sqrt{n\varepsilon})^2}{kT}\right], \qquad (2)$$

where $\varepsilon=mV_{cm}^2/2$ is the kinetic energy of a carbon atom moving with the precursor CM velocity V_{cm}. For low V_{cm} values with $n\varepsilon \ll kT$ (or $\sqrt{n\varepsilon/E} \ll 1$ for $E \geq kT$) the flux-energy distributions of the C_n groups [Eq. (2)] are practically the same for all n with most probable energies $E_{mp} \approx kT$. In the opposite case with high V_{cm} values ($n\varepsilon > kT$) one gets different shifted distributions with $E_{mp} \approx n\varepsilon$. In the following, we will show that Eq. (2) can describe all the experimental KEDs for both Ψ=45° and Ψ=135° reasonably well using only a single pair of fitting parameters (kT, ε) for all KEDs within a given E_o value.

First we will test this model using the formerly measured C_n^- KEDs under near-grazing (Ψ=45° and θ_i=63±1°) configuration.[12,13] These measurements were discussed before only in terms of most probable energies but no attempt was made at analyzing the complete KEDs shape. Figure 2 shows the measured C_n^- KEDs for Ψ=45° and E_0=300 eV

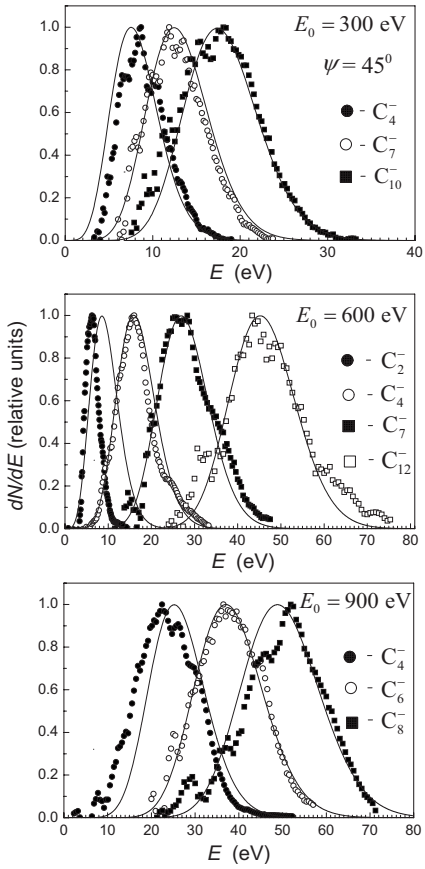

FIG. 2. Kinetic energy distributions of scattered C_n^- fragment anions following impact of C_{60}^- on a gold surface with energies E_0=300, 600, and 900 eV at near-grazing incidence (Ψ=45° and θ_i=63°). Both measured and calculated (lines) distributions are shown. A single pair of parameters (kT and ε) was best fitted (see text) for each E_0 value (family of distributions). All distributions are normalized to the same peak intensity.

(n=4,7,10), E_0=600 eV (n=4,7,12), and E_0=900 eV (n=4,6,8) together with calculated KEDs using Eq. (2). All distributions are normalized to the same peak value at the most probable energies.

All calculated C_n^- KEDs for a given E_0 value (a complete KEDs family) were simultaneously best fitted to the corresponding measured KEDs family. The resulted uniquely fitted pairs of parameters (kT, ε) for each family are $kT=0.51\pm0.07$ eV and $\varepsilon=1.63\pm0.10$ eV (V_{cm}=5210 m/s) for E_o=300 eV, $kT=0.65\pm0.06$ eV and ε=3.66±0.01 eV (V_{cm}=7810 m/s) for E_o=600 eV, and $kT=0.83\pm0.11$ eV and $\varepsilon=5.90\pm0.27$ eV (V_{cm}=9920 m/s) for E_o=900 eV. The spread of each parameter value is a mean one derived from the least-squares fitting of the calculated and measured KEDs separately for each n within a given KEDs family. The calculated KEDs families agree rather well, within relatively narrow spreads, with the measured ones (excluding the C_2^- KED for E_o=600 eV).

We now turn to analyze the near-normal KEDs measured here at Ψ=135°. The agreement obtained between measured and calculated [using Eq. (2)] KEDs of C_n^- fragments (n=4,6,9) for E_0=300 eV and 600 eV is presented in Fig. 1. Again, the pair of parameters (kT, ε) is best fitted for each complete family of KEDs corresponding to a given E_0 value. The values obtained are $kT=0.68\pm0.08$ eV and ε=0.032±0.023 eV (V_{cm}=730 m/s) for E_o=300 eV and $kT=0.64\pm0.07$ eV and $\varepsilon=0.01\pm0.01$ eV (V_{cm}=410 m/s) for E_o=600 eV. The agreement between calculated and measured KEDs is again quite good. The trend for increased width of the KEDs with increase in fragment size n is well reproduced by the calculation. Note that although the velocity V_{cm} (as given by the fitted ε value) is very small for Ψ=135° collisions, trying to fit the KEDs in Fig. 1 (E_o=300 and 600 eV) using ε=0 will result in a broader mass-independent Maxwellian distribution (with $E_{mp}=kT$=1.3 eV) which cannot reproduce the mass-dependent variation in the measured KEDs. For the near-grazing scattering at Ψ=45°, the kT value of the outgoing precursor ensemble of carbon atoms increases from 0.51 to 0.83 eV with increase in E_0 from 300 to 900 eV. The kinetic energy loss of the scattered precursor is ~0.6 E_0. However, for Ψ=135°, when the relative kinetic energy loss is nearly 100%, the parameter kT practically does not change and even slightly decreases with E_0, from 0.68 eV for E_0=300 to 0.64 eV for E_0=600. Note that for Ψ=135° the precursor kinetic energy also decreases with E_0, namely. $60\varepsilon\approx1.9$ eV for E_0=300 eV and ≈0.6 eV for E_0=600 eV. It can be argued that in this case the disintegration event is completed "during collision" while the departing C_n fragments are still in close contact with the surface. Estimating the fragmentation distance from the surface $Z(n)=\Delta l[V_{cm}\cos\theta_r/\overline{V_{rel}(n)}]$ [with $\overline{V_{rel}(n)}$ as the average relative velocity of fragmenting C_n groups and Δl as the characteristic increase in separation between these groups due to the fragmentation process] and assuming $\Delta l\sim2$ Å with $V_{cm}=\sqrt{2\varepsilon/m}$, $\overline{V_{rel}(n)}=\sqrt{16kT/\pi}$ nm we obtain for E_o=300 eV, $Z(4)$=0.51 Å and $Z(9)$=0.77 Å, and for E_o=600 eV, $Z(4)$=0.30 Å and $Z(9)$=0.45 Å. The subangstrom distance indeed implies that in this case the multifragmentation process occurs practically at the surface although there is a residual velocity correlation which gradually diminish with increase in E_o.

At E_0=900 eV the behavior of the KEDs family (see Fig. 1) can no longer be described in terms of an evaporating precursor, leaving the surface with some velocity V_{cm}. The trend observed for the KEDs width for the E_0=300 and 600 eV is now reversed. The distributions are getting narrower with increase in cluster size n from C_2^- to C_5^- but maintain a nearly constant width for C_5^- to C_9^-. This KED behavior closely resembles the behavior of KEDs of neutral clusters (in the range of $E\leq20$ eV) sputtered off metals under bombardment by Ar^+ ions with $E_0\approx3-5$ keV [see, for example, the KEDs of Al_n (Ref. 17) and Ag_n,[18] n=2–6]. Such similarity possibly points at similar mechanisms underlying the formation of both scattered C_n^- fragments and sputtered metallic clusters. One can suggest that under near-normal incidence of C_{60}^- ions the collision process begins by stopping of frontal C atoms (on the front C_{60} hemisphere) so that these atoms now serve as a new "target" atoms for the still propagating atoms at the back hemisphere. These still moving atoms transfer their impulse and energy to the "target" C atoms and sputter them as C_n^- clusters. This mechanism can be named "self-sputtering."[19]

The similar behavior observed for KEDs of scattered C_n^-

fragments under the C_{60}^- impact and KEDs (in the range of $E \leq 20$ eV) of neutral clusters sputtered from metals under atomic ion bombardment mentioned above suggests that the collision cascades induced in the metal following impact of few keV atomic ions can also be characterized by a "temperature" parameter. It is interesting to mention in this context that the KED behavior of sputtered clusters [e.g., Al_n (Ref. 17) and Ag_n (Ref. 18) as mentioned before] is still considered to be an unresolved issue. The correlation drawn here between the two (assumingly) related phenomena can therefore shed some light on this intriguing impact excitation/emission process.

Next, we would like to discuss the collisional internal energy excitation of the precursor species for the case of near-grazing incidence ($\Psi = 45°$). The average internal energy $\bar{E}_v$ of the highly vibrationally excited C_{60}^- precursor species can be evaluated in the equipartition limit via $\bar{E}_v = 174$ kT. Using the fitted kT values from Fig. 1, this expression leads to $\bar{E}_v - ZPE \equiv E_v^{\text{eff}} \approx 79$, 103, and 134 eV for $E_0 = 300$, 600, and 900 eV correspondingly (here ZEP is the C_{60} zero point energy and equals 9.7 eV).[20] These values of E_v^{eff} exceed (or are nearly the same as) the normal components of the kinetic energy loss of the precursor species calculated as $\Delta E_\perp(E_0) = [E_0 \cos^2 \theta_i - n\varepsilon(E_0) cos^2 \theta_r]$: 52, 103, and 152 eV correspondingly ($\theta_i = 63°$, $\theta_r = 72°$). Taking into account also an appreciable part β of $\Delta E_\perp$ which is lost to surface excitation, one gets $E_v^{\text{eff}} \gg (1-\beta)\Delta E_\perp(E_0)$, thus leading to the conclusion that a substantial part of E_v^{eff} is contributed by the parallel component of the kinetic energy loss $\Delta E_\parallel$. It is thus quite possible that the vibrational excitation is partly mediated by an efficient translational to rotational energy transfer as proposed earlier for the supersonically accelerated neutral C_{60} in the $E_0 = 10-40$ eV impact energy range.[21] A possible mechanism involves friction forces (due to some C_{60}-surface adhesive interactions) associated with a translational slip during the scattering process. These forces can generate a torque leading to C_{60} rotation and (asymptotically) to rolling without slipping.

In summary, we have observed two distinct multifragmentation modes following the surface impact of C_{60}^-: a post-collision event at near-grazing incidence with a common average velocity for all fragments and a during-collision event at near-normal incidence with a common average energy for all fragments. It was demonstrated that a transition between the two multifragmentation modes can be induced by varying the scattering angle. Using a unified approach and describing the disintegrating cluster (outgoing precursor) as a high-temperature highly confined hot "gas" of C_n groups moving with some CM velocity, we have reproduced all measured KEDs for the two (seemingly) different multifragmentation modes. In spite of the very different energy losses for the two scattering angles, the mutifragmentation event is found to be velocity correlated even for the near-normal incidence, where we observe a gradual increase in distribution width with the size of the C_n^- fragment. This tendency gradually weakens with impact energy till complete reversal while the system approaches an intrinsic self-sputtering behavior.

*Current address: Nanoscale Physics Research Laboratory, School of Physics and Astronomy, University of Birmingham, Birmingham B15 2TT, United Kingdom.

[1] *Fragmentation Phenomena*, Les Houches Series, edited by D. Beysens, X. Campi, and E. Pefferkorn (World Scientific, Singapore, 1995), and references therein.
[2] L. Oddershede, P. Dimon, and J. Bohr, Phys. Rev. Lett. **71**, 3107 (1993).
[3] J. P. Bondorf, A. S. Botvina, A. S. Iljinov, I. N. Mishustin, and K. Sneppen, Phys. Rep. **257**, 133 (1995).
[4] T. Raz, U. Even, and R. D. Levine, J. Chem. Phys. **103**, 5394 (1995).
[5] T. Raz and R. D. Levine, J. Chem. Phys. **105**, 8097 (1996).
[6] E. Hendell, U. Even, T. Raz, and R. D. Levine, Phys. Rev. Lett. **75**, 2670 (1995).
[7] H. Yasumatsu, S. Koizumi, A. Terasaki, and T. Kondow, J. Chem. Phys. **105**, 9509 (1996).
[8] B. Kaiser, T. M. Berhnhardt, B. Stegemann, J. Opitz, and K. Rademann, Phys. Rev. Lett. **83**, 2918 (1999).
[9] D. G. Schultz and L. Hanley, J. Chem. Phys. **109**, 10976 (1998).
[10] J. Laskin, T. H. Bailey, and J. H. Futrell, J. Am. Chem. Soc. **125**, 1625 (2003).
[11] R. D. Beck, C. Warth, K. May, and M. M. Kappes, Chem. Phys. Lett. **257**, 557 (1996); R. D. Beck, J. Rockenberger, P. Weis, and M. M. Kappes, J. Chem. Phys. **104**, 3638 (1996).
[12] A. Bekkerman, A. Kaplan, E. Gordon, B. Tsipinyuk, and E. Kolodney, J. Chem. Phys. **120**, 11026 (2004).
[13] A. Kaplan, A. Bekkerman, E. Gordon, B. Tsipinyuk, M. Fleischer, and E. Kolodney, Nucl. Instrum. Methods Phys. Res. B **232**, 184 (2005).
[14] E. E. B. Campbell and F. Rohmund, Rep. Prog. Phys. **63**, 1061 (2000), and references therein.
[15] S. Wethekam and H. Winter, Phys. Rev. A **76**, 032901 (2007).
[16] T. Matsushita, K. Nakajima, M. Suzuki, and K. Kimura, Phys. Rev. A **76**, 032903 (2007).
[17] S. R. Coon, W. F. Calaway, M. J. Pellin, G. A. Curlee, and J. M. White, Nucl. Instrum. Methods Phys. Res. B **82**, 329 (1993); The width of the kinetic energy distributions is largest for Al_2 and is gradually decreasing in the order $Al_2 > Al_3 > Al_4$ and then remains practically constant for Al_4, Al_5, and Al_6 ($E \leq 20$ eV).
[18] M. Wahl and A. Wucher, Nucl. Instrum. Methods Phys. Res. B **94**, 36 (1994); The width of the kinetic energy distributions is largest for Ag_2 and is gradually decreasing in the order $Ag_2 > Ag_3 > Ag_4$ and then remains practically constant for Ag_4, Ag_5, and Ag_6 ($E \leq 8$ eV).
[19] A clear distinction should be made between the (intrinsic) self-sputtering process as proposed here (in the sense that the cluster projectile sputters itself during collision) and the sputtering of a metal target by an incident atomic ion of the same element. (e.g., Ag target sputtered by incident Ag^+ ions). The last event is also described in the literature as "self-sputtering."
[20] B. Tsipinyuk, A. Budrevich, M. Grinberg, and E. Kolodney, J. Chem. Phys. **106**, 2449 (1997).
[21] E. Kolodney, B. Tsipinyuk, A. Bekkerman, and A. Budrevich, Nucl. Instrum. Methods Phys. Res. B **125**, 170 (1997).